

Faulted Branch Identification on Power Distribution Systems Under Noisy Environment

Karen Rezende Caino de Oliveira, Rodrigo Hartstein Salim, Adalberto Shuck Jr., Arturo Suman Bretas

Abstract—Faulted branch identification is extremely important for power distribution systems operation and restoration. Also, noisy environments are common in substations, where the relays are normally installed. In this paper a novel formulation that estimates the faulted section of an unbalanced power distribution system considering a noisy environment is presented. The method uses travelling waves and autocorrelation theory, and was developed using only local voltage data. The encouraging results demonstrate the technique’s high precision in determining faulted branches considering faults without resistance.

Index Terms—Fault diagnosis, Fault location, Power system transients, Correlation, Power distribution faults.

I. INTRODUCTION

PROTECTION schemes philosophy in power distribution systems (PDS) is to remove faulted lines (and equipments) after the detection of a permanent fault. After protection scheme’s operation, maintenance crew try to heal these faulted lines as fast as possible, in order to restore the system without seriously affecting its reliability. To achieve this objective, a precise fault location estimate must be provided.

For years the maintenance crews of distribution companies executed the fault location (FL) process through visual inspection along the overhead lines. Other techniques used were based on brute force methods, such as restoration through switching and phone calls from consumers [1]. Due to the large amount of laterals and the unbalanced nature of current PDS, the cited LF methods present low efficiency, which, in turn, results in the reduction of system reliability and in the increase on operational costs. With the development of digital protection systems, it became possible the usage of automated FL methods.

The main difference between FL methods and faulted branch identification (FBI) methods is that the latter results only in a faulted region. In PDS, FBI methods are very well suited, since each branch of the system may correspond to only a few meters. In this systems, FBI methods can also be

used as part of FL algorithms, helping them to select only one fault location among several expected estimates [2]–[4].

In the recent years, several FBI methodologies were developed for PDS [3], [5]–[8]. However, these existing methodologies are not robust to several practical aspects regarding the power protection operation, such as the existence of laterals [7] and the PDS operation characteristics [5], [6]. Also, none of the cited methods presents a consideration on noisy environments, which are common in power distribution substations, where the digital protection relays are normally located [9].

Considering the above mentioned limitations of current FBI methods, this work presents an FBI methodology for PDS. The main objective of this work is to propose an efficient method, with high precision and low operation cost. In this way, the proposed methodology requires only local voltage measurements, available at the substation, and is based on traveling waves and autocorrelation theory. The methodology was developed on Matlab and results are obtained for a modified version of the IEEE 13 Node Test Feeder, whose faults were simulated on EMTP-RV software [10].

The remaining of this paper is presented as follows: Section II describes and discusses the proposed formulation. Section III describes the case study system. Section IV presents the results obtained in the case study system. The discussions and conclusions are presented in Section V.

II. PROPOSED METHODOLOGY

The proposed methodology requires only three-phase local voltage (at the substation terminals) and system data: line and cable models, loads and system topology. It is divided into four subroutines, as shown in Fig. 1:

- *Low Frequency Filtering*: The low frequency components are filtered from the signal;
- *Modal Decomposition*: The high frequency three-phase voltage components are decoupled into three independent systems;
- *Travelling Waves Analysis*: The aerial mode transient signal is analysed using an autocorrelation algorithm in order to solve the faulted branch identification problem;
- *Propagation to the Next Branch*: The voltage signal is analyzed in several buses, using the *Travelling Waves Analysis* subroutine.

The *Travelling Waves Analysis* subroutine is actually the one that identifies the faulted branch. It has two internal routines, which comprise the estimation of the total branch propagation time and the fault induced transients propagation time. Using these two estimates, it is possible to determine the

This work was supported by Conselho Nacional de Desenvolvimento Científico e Tecnológico (CNPq) and Fundação de Amparo à Pesquisa do Estado de São Paulo (FAPESP).

K. R. Caino de Oliveira and R. H. Salim are with the University of São Paulo (EESC-USP), São Carlos, SP, Brazil, 13566-590 (e-mail: caino@sel.eesc.usp.br, salim@sel.eesc.usp.br, phone: +55 16 33739366 R. 219).

A. Shuck Jr. and A. S. Bretas are with the Federal University of Rio Grande do Sul (UFRGS), Porto Alegre, RS, Brazil, 90035-190 (e-mail: shuck@ufrgs.br, abretas@ece.ufrgs.br).

faulted branch with precision. The formulation is presented for faults without resistance, and also considers white noise in the analyzed signal. Each one of the subroutines are presented in details in the following subsections.

A. Low Frequency Filtering

This subroutine filters low frequency components of the three-phase voltage signals. It is required that this process does not interfere in the signal's phase, as its use is necessary in the following subroutines to determine the traveling waves propagation time on the distribution line.

The Butterworth filter is the one used in this work. This filter is designed to have a frequency response with no ripples in the passband. These filters have a magnitude changing related to the frequency characteristic. Thus, to implement this subroutine a bilinear transform was used. In order to implement the stopband necessary, a third order *Butterworth* filter was used.

Due to the high frequency range present in transients induced by faults on short lines [11], a cut off frequency, ω_c , equal to 50 kHz is used in this work.

B. Modal Decomposition

With the transient voltage signal filtered, the modal decomposition subroutine begins. As distribution systems lines are normally asymmetric, the modal transformation matrix components are not real and constant. This subroutine performs the modal transformation at the fault dominant frequency in order to eliminate its frequency dependency and to consider only the traveling waves due to the fault.

First, the transient signal dominant frequency is estimated. This estimate is used in the line's parameters calculation, at the fault dominant frequency. The dominant frequency is defined as the higher relative frequency component of the fault voltage signal. This estimate, F_P , is obtained by analyzing the transient signal through a Fourier Transform (FT). First the filtered voltage signals are transformed in the frequency domain through a FT. Then, F_P is chosen as the frequency component with highest absolute value.

Using F_P , the line parameters, Z_f and Y_f , are calculated. These values vary sharply with the frequency, estimating an erroneous wave time travel if calculated, on the algorithm, with any different frequency [12], [13]. With Z_f and Y_f , the modal transformation matrix is calculated through (1):

$$\mathbf{P} = [p_1 \quad p_2 \quad \cdots p_n], \quad (1)$$

where p_i are eigenvectors associated with the eigenvalues of the product $Z_f \cdot Y_f$.

Through matrix \mathbf{P} the modal transformation is performed [14] as defined in (2):

$$V(x, s) = \mathbf{P}\bar{V}(x, s), \quad (2)$$

where \bar{V} is the voltage vector in modal components, V_0 , V_α , V_β .

Still, the modal propagation matrix, $\bar{\gamma}$, is calculated from the parameters Z_f and Y_f as described in 3:

$$[\bar{\gamma}] = (\mathbf{P}^{-1}(Z_f Y_f)\mathbf{P})^{1/2}, \quad (3)$$

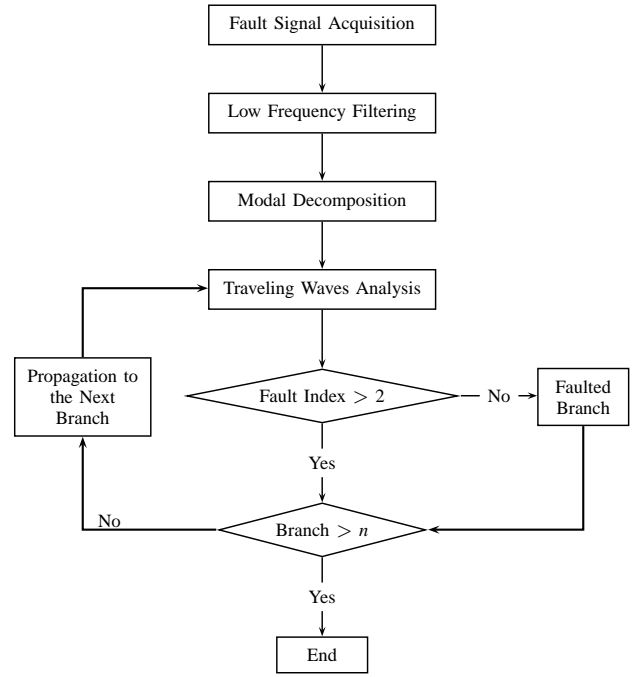


Figure 1. Proposed methodology.

where $\bar{\gamma}$ contains the traveling waves behavior in their three propagation modes.

C. Traveling Waves Analysis

This subroutine is divided into 3 processes: branch's total propagation time, waves traveling time due to faults and branch analysis through the *fault index*.

1) *Branch's Total Propagation Time*: For the branch's total wave time propagation estimate, the aerial mode has been used since it presents a low surge impedance variation with the frequency increase. This implies in a low variation of the overvoltage at the faulted phase [15].

Figure 2 illustrates the incident waves due to a fault occurrence in a distribution line, where:

$$\begin{array}{ll} V_1^- & \text{regressive incident wave} \\ V_1^+ & \text{progressive incident wave} \end{array}$$

The fault induced voltages at terminals A and B, are

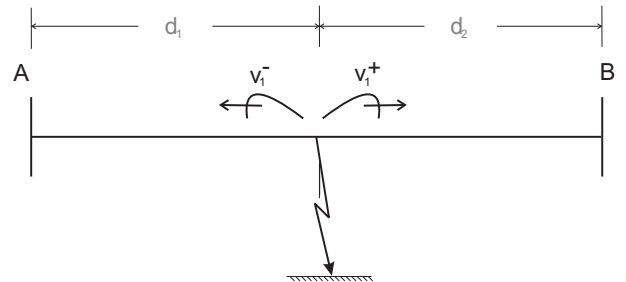


Figure 2. Faulted branch and the fault induced voltages

respectively given by:

$$V_{A1}(s) = e^{\gamma_1(s)d_1} \cdot V_1^- \quad (4)$$

$$V_{B1}(s) = e^{-\gamma_1(s)d_2} \cdot V_1^+ \quad (5)$$

With $V_1^+ = -V_1^-$ [15]:

$$-V_{A1}(s)e^{-\gamma_1(s)d_1} = e^{\gamma_1(s)d_2}V_{B1}(s) , \quad (6)$$

which yields that

$$V_{B1}(s) = -\frac{V_{A1}(s)e^{-\gamma_1(s)d_1}}{e^{\gamma_1(s)d_2}} . \quad (7)$$

Calculating γ_1 at the dominant frequency introduced by the fault in the transient state, V_{B1} yields:

$$V_{B1}(s) = -V_{A1}(s)e^{-\gamma_1(d_1+d_2)} . \quad (8)$$

Finally, using the inverse Laplace Transform in (8), and defining that the total section length is $L = d_1 + d_2$, the fault induced voltage at bus B in the time-domain is obtained by:

$$v_{B1}(t) = -v_{A1}(t)e^{-\gamma_1 \cdot L} \quad (9)$$

Equation (9) shows that the voltage induced by the fault at terminal B is equal to the terminal A voltage multiplied by a propagation factor. This adds to the traveling wave an amplitude attenuation, e^α , and an angle displacement, $e^{j\beta}$, since $\gamma_1 = \alpha + j\beta$, which is the aerial component of the propagation matrix, $\bar{\gamma}$, calculated at the *Modal Decomposition* subroutine.

Thus, the propagation time estimate, t_b , in the studied branch, is calculated through a simple relation between the angle displacement and the signal's cycle time, as given in (10):

$$t_b = \frac{16.7 \cdot 10^{-3} \cdot \beta L}{2\pi} \quad (10)$$

2) *Waves Traveling Time Due To Faults*: This process estimates the incident wave traveling time starting when it reflects on the measurement terminal, then reflects on the fault and returns to the measurement point (t_a). The Bewley-Lattice diagram in Figure 3 illustrates the reflections and refractions in a faulted branch with no fault resistance, between any two buses X and Z. According to the diagram, t_a can be calculated by (11):

$$t_a = 2 \cdot t_Z . \quad (11)$$

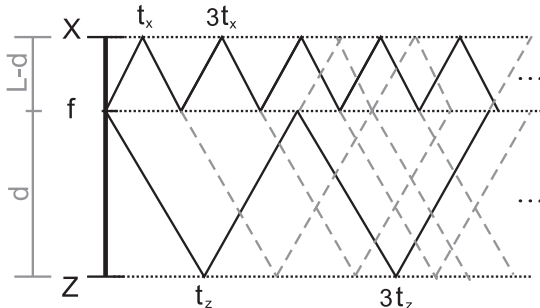


Figure 3. System's diagram with reflections and refractions due to a fault occurrence

Since this work is developed for faults without resistance, the transmission coefficient from terminal Z until terminal X, Γ_t , can be obtained by:

$$\Gamma_t = \frac{2 \cdot Z_{eq}}{Z_{eq} + Z_{line}} = 0 , \quad (12)$$

where Z_{eq} is the equivalent impedance of the branches involved in the discontinuity and Z_{line} is the line impedance.

Thus, for a fault without resistance, the incident wave is fully reflected at the fault location and returns to the measurement terminal. This ensures that the first two successive waves to arrive at Z are: the incident wave and its reflection on the fault location. As the regressive incident wave also fully reflects in the fault, its components are not seen in the measurement point at the local feeder.

To identify the arrived waves, an autocorrelation estimator is used, measuring the similarity's degree of the signal with itself. Within the transient signal it is possible to identify the first incident wave that arrives to the terminal and the wave reflected at the fault point. Equation (13) defines the autocorrelation estimator:

$$\bar{r}[k] = \frac{1}{N - |k| - 1} \sum_{n=1}^{N-|k|-1} v_{1F}[n]v_{1F}[n - k] , \quad (13)$$

for $-N \leq k \leq N$, where:

$\bar{r}[k]$	autocorrelation estimator
v_F	faulty phase F modal voltage
N	number of signal samples
k	temporal displacement

The autocorrelation eliminates the signal's noise, and outputs values representing the correlated signals. These components are normalized and expressed as equally spaced pulses that represent the traveling waves due to faults. From the samples number between two similar voltage waves, given by N, the wave traveling time, t_a , is obtained through (14):

$$t_a = \frac{F_s}{N} , \quad (14)$$

where F_s is the signal's sampling frequency.

3) *Fault Branch Analysis*: For the fault branch analysis, it is used a *fault index*, k . This index expresses a relation between the waves travel time due to the fault, t_a , and the total branch propagation, t_b , which is illustrated in Figure 3 and defined in (15). The k index is calculated by the ratio given in (16) and is used to determine if the analysed branch contains a fault.

$$t_B = t_Z + t_X \quad (15)$$

$$k = \frac{t_a}{t_b} . \quad (16)$$

Figure 3 also illustrates that if the analyzed branch is subjected to a fault, k will always be less than or equal to 2, as the relative propagation time due to a fault, t_a can not be greater than two times the branch's propagation time, t_b . Calculated this index, the algorithm defines the branch status (faulted or not), and then estimates the downstream bus voltage.

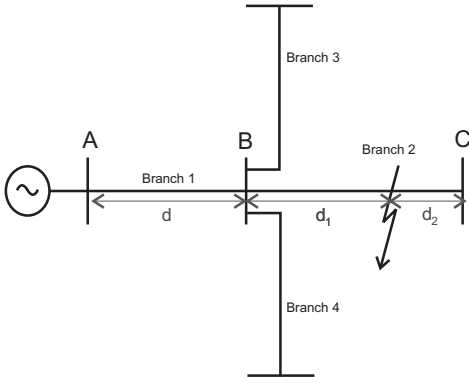


Figure 4. Branched system

D. Propagation to the Next Branch

In order to account for systems laterals, the proposed algorithm calculates the fault index in every branch of the analyzed PDS. After the k index is calculated for every branch, possible faulted branches are yielded by the algorithm. Figure 4 illustrates a PDS in order to demonstrate the method propagation process.

The idea is to change the system observer by translating the measured voltage signals to all the system's busbars, starting from the substation voltage measurements. This is executed with use of the propagation theory, thus not requiring remote measurements from other nodes besides the feeder substation. From (9) and according to Figure 4, v_{C1} can be defined by 17:

$$v_{C1}(t) = -v_{B1}(t)e^{-\gamma_1^{(2)} \cdot L}, \quad (17)$$

where $L = d_1 + d_2$, and the index (2) represents the aerial propagation matrix component at branch 2. Thus, the total branch propagation time, t_b , is estimated through (10). With (17) it is possible to calculate the voltages in one node using only the voltages at another node and the system parameters. Starting this procedure from the substation, the voltages in every node upstream to the faulted branch can be precisely calculated.

Still, to perform the autocorrelation and to estimate the waves traveling time due to faults, t_a , the voltage signal reference is propagated to bus B, where the signal finds a discontinuity. In order to estimate the downstream bus voltage, it is necessary to calculate a transfer matrix, Γ_t , that as well as the line's propagation, also adds a delay to the signal waves traveling time.

With the transfer modal matrix calculated, $\overline{\Gamma}_t$, the signal v_{B1} is calculated, with (19), to be used as the autocorrelation input, where t_a is estimated:

$$v_{A1} = \overline{\Gamma}_t \cdot v_{B1} \cdot e^{\gamma_1 \cdot d} \quad (18)$$

$$v_{B1} = \frac{v_{A1}}{\overline{\Gamma}_t} \cdot e^{-\gamma_1 \cdot d}. \quad (19)$$

III. CASE STUDY

The case study system is the *IEEE 13 Node Test Feeder* system [16]. This system was chosen due to its topological and operational characteristics as it also serves as reference

Table I
BRANCHES DATA

Bus A	Bus B	Length [m]	Config.
632	645	152.4	603
632	633	152.4	602
633	634	0	XFM-1
645	646	91.44	603
650	632	609.6	601
684	652	243.84	607
632	671	609.6	601
671	684	91.44	604
671	680	304.8	601
671	675	304.8	606
684	611	91.44	605

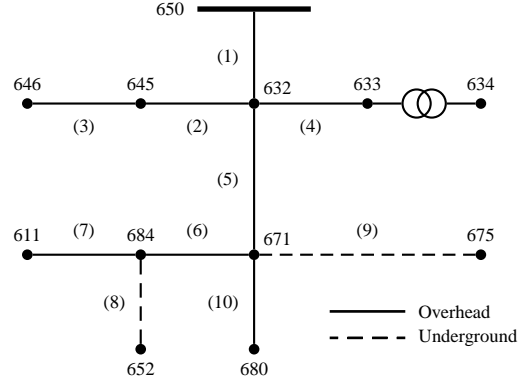


Figure 5. Modified IEEE 13 Node Test Feeder.

for harmonic propagation studies [17]. Figure 5 illustrates the case study. Table I presents the changes inserted into the IEEE 13-bus test node feeder system's line configuration. Still, its configuration presents two-phase, three-phase and single-phase lines, shunt capacitors, and distributed loads. These are connected in Δ and Y configurations.

Two different line models were used in DCG's EMTP software [10], one for the overhead lines and other for the underground cables, due to their specific characteristics. The overhead lines were modeled as frequency dependent parameters [18]. On the other hand, the underground cables were modeled using the FDQ model [19], which includes not only the cable parameters dependency on frequency, but also the modal transformation matrix (Q -matrix) frequency dependency. The FDQ model was chosen since the Q -matrix of underground cables strongly depends on frequency, and constant-transformation-matrix models generally produce very poor results.

IV. RESULTS

In order to evaluate the proposed algorithm's performance, simulated faults were analyzed, considering the benchmark system. The system branches were enumerated as shown in Fig. 5. Single line-to-ground (SLG) faults without resistance were simulated in each of the branches, under different fault locations and faulted phases, totalizing 123 fault cases. The fault points all have a minimum distance of 40m to the nodes and loads (discontinuities), due to the large computational

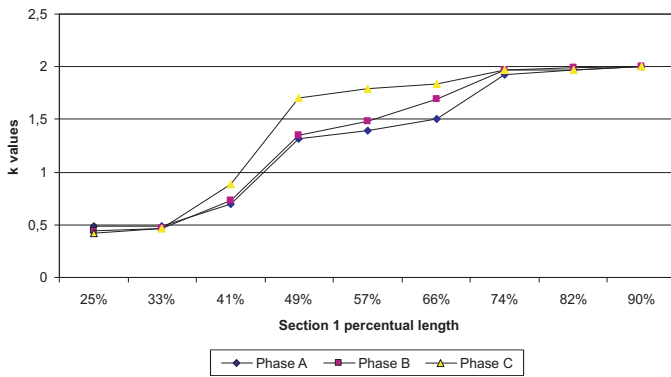


Figure 6. Values assumed by k for faults in different phases on branch 1.

effort needed to simulate faults closer to them. Each simulated fault was analyzed through the proposed algorithm considering voltage signals without noise (directly from the simulations) and also considering a 40 dB (SNR) white noise, introduced via Matlab in the voltage signals.

In all analyzed faults the methodology yielded the correct faulted branch, with or without noise. The only mistake occurred for a fault located at 550m from the measurement bus (650), in both noisy and non noisy cases. In this case, the fault was very near node 632 (50m), a discontinuity. In this case, the algorithm yielded two faulted branches: 1 and 5. The occurrence of this type of error may be a consequence of the line and system configuration of both branches (1 and 5). Both of them have the same line geometry and length. In this way, for faults near the node between them, the algorithm yields a fault index (k) that is near 2 for branch 1 and near zero for branch 5.

Another important analysis concerns the fault index variation when the fault location is kept constant and the faulted phase is varied. Theoretically, in fully balanced systems (loads and line geometry), the fault index should not vary for faults at the same distance, even if in different phases. Since the analyzed system is highly unbalanced (loads and line geometry), the values assumed by this index are different for faults at the same location and in different phases. Fig. 6 shows the values assumed by k for faults simulated in different phases on branch 1.

In this Figure, it is possible to verify that for faults on phase C near the middle of branch 1 (50%), the fault index assumes a very large value, where it should be next to 1. This is a situation where there are distributed loads along the line, introducing a discontinuity with unbalanced load.

V. DISCUSSIONS AND CONCLUSIONS

This paper presents a new formulation for fault branch identification on unbalanced distribution systems under noisy environment. The proposed methodology aims to reduce the system's restoration time and yet to complete existent fault location algorithms.

The proposed method uses as input only local voltage data having a low implementation cost on PDS. The algorithm was implemented under MATLAB software and tested with simulations obtained in DCG's EMTP-RV program. A 40 dB

white noise was introduced in the signals to simulate the noisy environment. The studied system was the modified IEEE 13 Nose Test Feeder.

Tests results demonstrate the accuracy and robustness of the technique and its precision in identifying faulted branches considering faults without resistance under noisy environment. However, efforts must have to be done prior to a practical implementation, in relation to faults with resistance.

VI. REFERENCES

- [1] K. Zimmerman and D. Novosel, "IEEE Guide for Determining Fault Location on AC Transmission and Distribution Lines," Piscataway, NJ, Tech. Rep. IEEE Std. C37.114-2004, 2005.
- [2] J. Zhu, D. L. Lubkeman, and A. A. Girgis, "Automated fault location and diagnosis on electric power distribution feeders," *IEEE Trans. Power Del.*, vol. 12, no. 9, pp. 801–809, 1997.
- [3] S.-J. Lee, M.-S. Choi, S.-H. Kang, B.-G. Jin, D.-S. Lee, B.-S. Ahn, N.-S. Yoon, H.-Y. Kim, and S.-B. Wee, "An intelligent and efficient fault location and diagnosis scheme for radial distribution systems," *IEEE Trans. Power Del.*, vol. 19, pp. 524–532, 2004.
- [4] R. H. Salim, K. R. C. Oliveira, M. Resener, A. D. Filomena, and A. S. Bretas, "Hybrid fault diagnosis scheme implementation for power distribution systems automation," *IEEE Trans. Power Del.*, vol. 23, no. 4, pp. 1846–1856, Oct. 2008.
- [5] Y.-Y. Hsu, F.-C. Lu, Y. Chien, J. Liu, J. Lin, P. Yu, and R. Kuo, "An expert system for locating distribution system faults," *IEEE Trans. Power Del.*, vol. 6, no. 1, pp. 366–372, 1991.
- [6] S.-J. Huang, "Application of immune-based optimization method for fault-section estimation in a distribution system," *IEEE Trans. Power Del.*, vol. 17, no. 3, pp. 779–784, 2002.
- [7] H. Hizam, P. A. Crossley, P. Gale, and G. Bryson, "Fault section identification and location on a distribution feeder using travelling waves," *Power Engineering Society Summer Meeting*, vol. 3, pp. 1107–1112, 2002.
- [8] K. R. C. Oliveira, R. H. Salim, M. Resener, A. D. Filomena, and A. S. Bretas, "Unbalanced underground distribution systems fault detection and section estimation," *Lecture Notes in Computer Science*, vol. 4682, pp. 1054–1065, 2007.
- [9] A. G. Phadke and J. S. Thorp, *Computer Relaying for Power Systems*. Research Studies Press LTD., 1994.
- [10] Development Coordination Group, *Electromagnetic Transient Program: EMTP-RV*, 2006.
- [11] G. W. Swift, "The spectra of fault-induced transients," *IEEE Trans. Power App. Syst.*, vol. PAS-98, pp. 940–947, 1979.
- [12] J. A. Martinez, B. Gustavsen, and D. Durbak, "Parameter determination for modeling system transients—Part I: Overhead lines," *IEEE Trans. Power Del.*, vol. 20, pp. 2038–2044, 2005.
- [13] B. Gustavsen, J. A. Martinez, and D. Durbak, "Parameter determination for modeling system transients—Part II: Insulated cables," *IEEE Trans. Power Del.*, vol. 20, pp. 2045–2050, 2005.
- [14] C.-T. Chen, *Linear System Theory and Design*. Oxford University Press, 1999.
- [15] A. Greenwood, *Electrical transients in power systems*. Wiley-Interscience, 1971.
- [16] W. Kersting, "Radial distribution test feeders," in *Proc. IEEE Power Engineering Society Winter Meeting*, vol. 2, 2001, pp. 908–912 vol.2.
- [17] *Test Systems for Harmonics Modeling and Simulation*, IEEE Power Engineering Society, New York, USA, 1998. [Online]. Available: <http://www.pes-psrc.org/>
- [18] J. Marti, "Accurate modelling of frequency-dependent transmission lines in electromagnetic transient simulations," *IEEE Trans. Power App. Syst.*, no. 1, pp. 147–157, Jan. 1982.
- [19] L. Marti, "Simulation of transients in underground cables with frequency-dependent modal transformation matrices," *IEEE Trans. Power Del.*, vol. 3, no. 3, pp. 1099–1110, July 1988.